British Journal of Pharmacology (1999) 126, 251–263 
http://www.stockton-press.co.uk/bjp

# Effects of phrixotoxins on the Kv4 family of potassium channels and implications for the role of $I_{to1}$ in cardiac electrogenesis

[1]Sylvie Diochot, [1]Milou-Daniel Drici, [1]Danielle Moinier, [1]Michel Fink & *,[1]Michel Lazdunski

[1]Institut de Pharmacologie Moléculaire et Cellulaire, CNRS, 660 route des Lucioles, Sophia Antipolis, 06560 Valbonne, France

**1** In the present study, two new peptides, phrixotoxins PaTx1 and PaTx2 (29–31 amino acids), which potently block A-type potassium currents, have been purified from the venom of the tarantula *Phrixotrichus auratus*.

**2** Phrixotoxins specifically block Kv4.3 and Kv4.2 currents that underlie $I_{to1}$, with an $5 < IC_{50} < 70$ nM, by altering the gating properties of these channels.

**3** Neither are the *Shaker* (Kv1), *Shab* (Kv2) and *Shaw* (Kv3) subfamilies of currents, nor HERG, KvLQT1/IsK, inhibited by phrixotoxins which appear specific of the *Shal* (Kv4) subfamily of currents and also block $I_{to1}$ in isolated murine cardiomyocytes.

**4** In order to evaluate the physiological consequences of the Ito1 inhibition, mice were injected intravenously with PaTx1, which resulted in numerous transient cardiac adverse reactions including the occurrence of premature ventricular beats, ventricular tachycardia and different degrees of atrio-ventricular block.

**5** The analysis of the mouse electrocardiogram showed a dose-dependent prolongation of the QT interval, chosen as a surrogate marker for their ventricular repolarization, from $249 \pm 11$ to $265 \pm 8$ ms ($P < 0.05$).

**6** It was concluded that phrixotoxins, are new and specific blockers of Kv4.3 and Kv4.2 potassium currents, and hence of $I_{to1}$ that will enable further studies of Kv4.2 and Kv4.3 channel and/or $I_{to1}$ expression.

**Keywords:** Spider toxins; voltage-gated potassium channels; Ito; Kv4 channels; A-type current; electrocardiogram

**Abbreviations:** AV, atrio-ventricular; ECG, electrocardiogram; EIMS, electrospray ionization mass spectrometry; HPLC, high performance liquid chromatography; TFA, trifluoroacetic acid

## Introduction

Toxins isolated from animal venoms have been invaluable tools for probing the structure and function of potassium ($K^+$) channels from the Kv family (Aiyar *et al*., 1995; Bidard *et al*., 1987; Harvey & Anderson, 1991; Miller, 1995; Mockzydlowski *et al*., 1988; Pongs, 1992a; Rehm & Lazdunski, 1988; Strong, 1990; Swartz & McKinnon, 1997). Snake, bee, sea-anemone and scorpion toxins specifically target *Shaker* (Kv1) and *Shaw* (Kv3) related $K^+$ channel subfamilies (Bidard *et al*., 1987; Diochot *et al*., 1998; Garcia *et al*., 1994; Grissmer *et al*., 1994; Pongs, 1992b; Rehm *et al*., 1988; Schweitz *et al*., 1995) whereas newly isolated spider toxins are useful tools to analyse the *Shab* (Kv2) and *Shal* (Kv4) related $K^+$ channels, which are widely spread in mammalians cells (Sanguinetti *et al*., 1997; Swartz & McKinnon, 1997).

The *Shal* subfamily comprises three genes, Kv4.1, Kv4.2 and Kv4.3 that all express transient $K^+$ currents in heterologous systems (Baldwin *et al*., 1991; Pak *et al*., 1991; Serodio & Rudy, 1998). These genes are abundantly expressed in several types of central and peripheral neurons as well as in the heart, with differential topographic expression (Kaczmarek & Strumwasser, 1984; Segal *et al*., 1984; Serodio *et al*., 1994, 1996; Serodio & Rudy, 1998). Thus, while Kv4.1 has only been characterized in the central nervous system (Pak *et al*., 1991), Kv4.3 and Kv4.2 have also been located in the heart where their differential distribution, pharmacology and kinetics suggest that they are the molecular constituents of the transient $K^+$ current $I_{to1}$ (Barry & Nerbonne, 1996; Dixon *et al*., 1996; Yeola & Snyders, 1997). $I_{to1}$ modulates the action potential duration and/or shape (Barry *et al*., 1995; Barry & Nerbonne, 1996; Dixon & McKinnon, 1994; Dixon *et al*., 1996) and has a prominent role in mammalian heart cells by counterbalancing the fast inward sodium ($Na^+$) current in phase 1 of the action potential. Furthermore, the myocardial regional gradient of $I_{to1}$ participates in the fact that epicardial layers are the fastest to repolarize (Litovsky & Antzelevitch, 1987; Wettwer *et al*., 1994).

This paper describes the purification, structure and properties of two new toxins, phrixotoxins PaTx1 and PaTx2, that have been isolated from the venom of the Chile fire tarantula *Phrixotrichus auratus*. These toxins proved to be specific and potent blockers of the Kv4.3 and the Kv4.2 channels, as well as of the $I_{to1}$ current in rat isolated ventricular myocytes. They have been used to analyse the exact contribution of the $I_{to1}$ current in the cardiac function of mice.

## Methods

### *Purification of phrixotoxins*

The venom from *Phrixotrichus auratus* (Araneae, Theraphosidae) was purchased from Spider Farm (Feasterville, PA, U.S.A.). In a first screening attempt, we identified inhibitory activities of diluted venom (1 : 1000) for Kv4.3 currents among several representatives of $K^+$ channels tested, and purified the responsible peptides.

* Author for correspondence.

Active components were purified on a C18 reverse phase high performance liquid chromatography (HPLC) column using an aliquot of crude venom (12.5 mg). Lyophilized venom was diluted to 1.25 ml with 0.1% aqueous trifluoroacetic acid (TFA) and centrifuged at 4500 r.p.m. for 15 min. The supernatant was filtered through 0.22 $\mu$m filters (Millex GV4) and fractionated on a Beckman ODS C18 reversed-phase HPLC column ($10 \times 250$ mm) equilibrated in 85% solvent A (0.1% TFA in water) 15% solvent B (0.1% TFA in acetonitrile). Linear gradients of solvent B were used, at a flow rate of 1 ml $min^{-1}$. The UV absorbance of the effluent was monitored at 220 nm and 280 nm. The active fractions PaE and PaF were further purified on a TSK SP-5PW cation-exchange column ($7.5 \times 75$ mm) equilibrated in 100% of solvent C (1% acetic acid in water). The final purification step for the fractions PaE5 and PaF4 was carried out on a Waters Symmetry C18 reversed phase column ($4.6 \times 250$ mm) equilibrated in 10% of solvent B and 90% of solvent A.

### *Peptide sequencing and mass determination*

Lyophilized E5 and F4 peptides were reduced with 2-mercaptoethanol and pyridylethylated with 4-vinylpyridine before sequencing. They were submitted to Edman degradation on an Applied Biosystems model 477 A microsequencer. Molecular weights were determined by electrospray ionization mass spectrometry (EIMS).

### *Cell cultures and transfection*

Two days before transfection COS M6 cells were plated at a density of 20,000 on cover glasses and transfected by a modification of the DEAE-dextran/chloroquine method using 0.05 $\mu$g of super coiled pCI-Kv4.n plasmid DNA. A CD8-expressing plasmid (0.02 – 0.1 $\mu$g) was added in all transfection experiments to visualize transfected cells using anti-CD8 antibody-coated beads (Jurman *et al*., 1994). Currents were recorded within 1 – 2 days following transfection.

### *Plasmid constructions*

pBluescript-Kv4.1 (GenBank accession number M64226), Kv4.2 (GenBank accession number S64320) and Kv4.3 (GenBank accession number U75448) constructs were kindly provided by Drs L. Salkoff (Pak *et al*., 1991), L. Jan (Baldwin *et al*., 1991) and D. McKinnon (Dixon *et al*., 1996) respectively. The *Sal*I/*Not*I fragment excised from pBS-Kv4.1 and the *Xho*I/*Xba*I fragment excised from pBS-Kv4.3 were subcloned into the mammalian expression vector pCI (Promega Madison, Wisconsin, U.S.A.) to give pCI-Kv4.1 and pCI-Kv4.3. The entire coding sequence of Kv4.2 was amplified by PCR using a low error rate DNA polymerase (Pwo DNA polymerase, Boehringer Mannheim, Meylan, France) and subcloned into pCI vector to give pCI-Kv4.2. All constructs were characterized by restriction analysis and by a partial or complete sequencing on both strands by the dideoxy nucleotide chain termination method using an automatic sequencer (Applied Biosystems, model 373A).

### *Myocytes isolation*

The cell isolation was performed according to Mitra (Mitra & Morad, 1986). Briefly, the rat heart was excised and rapidly mounted on a modified Langendorff apparatus and subsequently perfused with Ca-free Tyrode solution containing 1.5 mg $ml^{-1}$ collagenase (type II, Sigma, 370 u $mg^{-1}$) and 50 $\mu$M $Ca^{2+}$ Tyrode. Pieces of ventricle were gently shaken and single myocytes were collected after filtration and stored at 4°C until use.

### *Electrophysiological measurements*

Electrophysiological measurements on COS transfected cells were performed 48 h after transfection using the whole-cell configuration of the patch-clamp technique. The pipette solution used for COS cells was (in mM): KCl 150, $MgCl_2$ 3, EGTA 5, HEPES-KOH 10 at pH 7.4. The pipette solution used for myocytes was (in mM): NaCl 10, KCl 136, $CaCl_2$ 0.5, EGTA 5, Mg-ATP 5, HEPES-KOH 5, at pH 7.4. The extra cellular solution composition for $K^+$ currents recordings in COS cells was (in mM): KCl 5, NaCl 150, $CaCl_2$ 1, $MgCl_2$ 3, HEPES-NaOH 1, pH 7.4. The extra cellular solution used for myocytes was (in mM): Choline Cl 135, KCl 5.4, $CaCl_2$, 2, $MgCl_2$ 1, Glucose 10, HEPES-KOH 10 at pH 7.4. $Cd^{2+}$ (0.5 mM) was added to block $Ca^{2+}$ currents. Bovine serum albumin 0.1% was added in toxin-containing solutions in order to prevent their adsorption.

The Kv4.2 and Kv4.3 current-voltage curves were determined by applying 10 mV incremental depolarizing pulses from a holding potential of $-80$ mV. Peak transient currents elicited by depolarizations, were measured after digital leak subtraction calculated at the end of depolarization (at 300 ms). All averaged data are presented as means $\pm$ s.e.mean.

### *Specificity of PaTx1 and PaTx2 for the Kv4.2 and Kv4.3 channels*

For screening purposes, *Xenopus* oocytes were injected with Kv1.1; Kv1.2; Kv1.3; Kv1.4; Kv2.1; Kv2.2; Kv3.1; Kv3.2; Kv3.4; Kv4.2; Kv4.3, and IRK1 complementary RNAs (cRNA) as described previously (Duprat *et al*., 1995). Currents were recorded 2 – 4 days following the injection using the two microelectrode voltage-clamp protocol. In order to determine the specificity of PaTx1 and PaTx2, increasing concentrations of toxins (100 nM to 1 $\mu$M), were applied on Kv1.n, Kv3.n, IRK1 currents expressed in *Xenopus* oocytes as well as on Kv1.5, Kv2.n, the background $K^+$ channel TREK-1, and the two components of the delayed rectifier, HERG and KvLQT1/Isk expressed in COS cells (Barhanin *et al*., 1996; Fink *et al*., 1996).

### *Animal electrophysiology*

We analysed the physiological effects associated with intravenous injections of increasing doses (0.1 – 40 nmol) of PaTx1 by measuring standard electrocardiographic parameters on anaesthetized Balb C mice, that were maintained on sterile regular rodent chow (R03, UAR, Epinay-France) and allowed free access to food and water in a facility at $21 \pm 1$°C with 12 h light/dark cycles.

### *Animal preparation for electrocardiography*

Twelve-week-old mice of both sexes, weighing 23 – 29 g, were studied. Mice were anaesthetized with sodium pentobarbital (SANOFI-France, 45 mg $kg^{-1}$ (i.p.) for the female adults and 55 mg $kg^{-1}$ (i.p.) for the male adults). Surface three-lead electrocardiograms (ECG) (bipolar lead DI, DII and DIII) were obtained by placement of dry electrodes carefully wrapped around each of the mouse four limbs. Respiratory and heart rates were continuously monitored during the procedure. A warning light was used to maintain body temperature within a range of $36 \pm 1$°C for prevention of hypothermia.

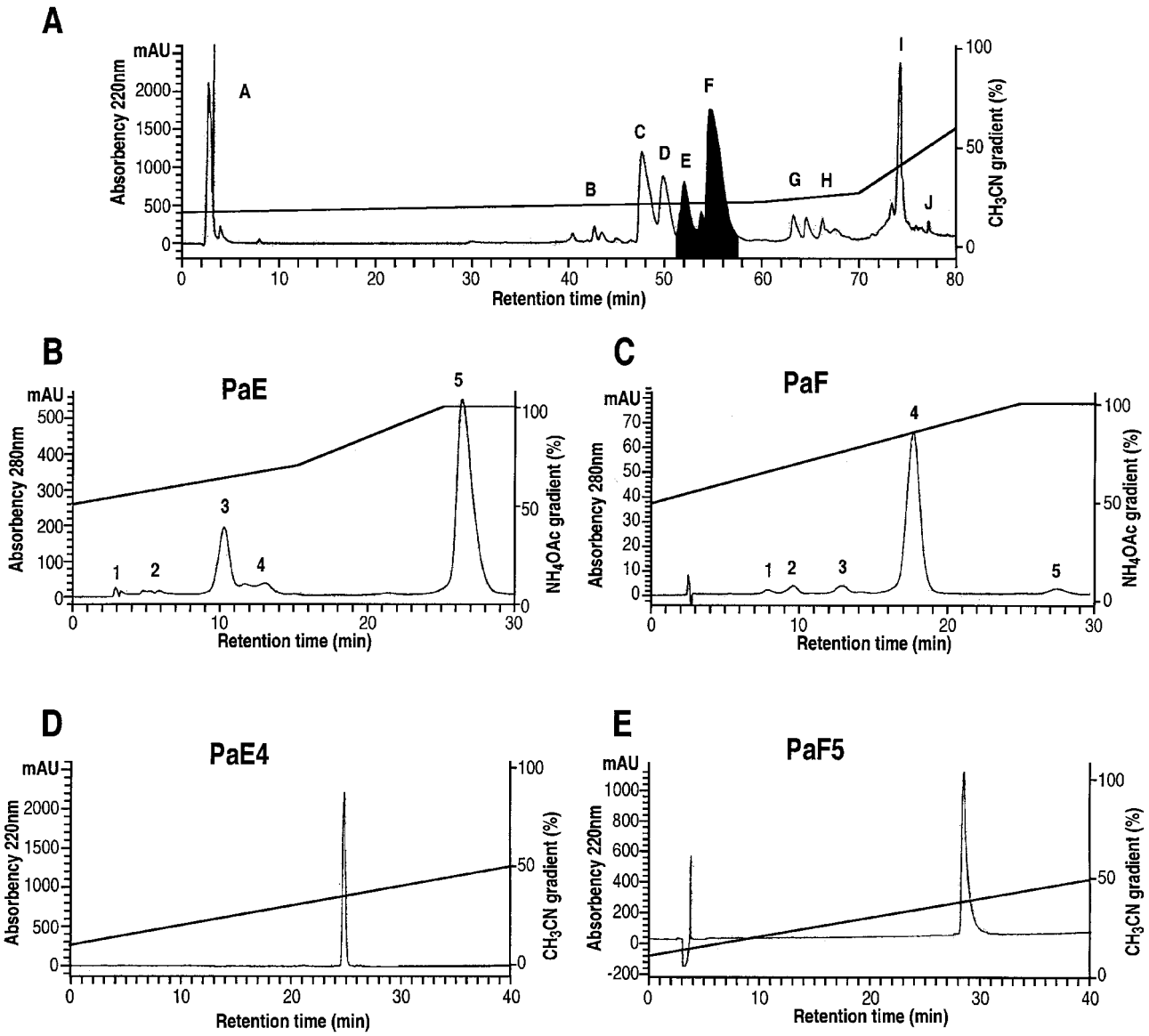


**Figure 1** Purification of phrixotoxins from *Phrixotricus auratus* venom. (A) Reverse phase HPLC chromatogram monitored at 220 nm illustrating the separation of 10 fractions – A – J – after loading 500 $\mu$l of diluted venom in a Beckman ODS C18 column. The stepwise solvent B (0.1% TFA in acetonitrile) gradient (from 15 – 30% over 60 min, from 30 – 35% over 10 min, then from 35 – 60% over 10 min) is indicated. Collected fractions E and F, active on Kv4.3 channels, are shaded. (B,C) Ion exchange chromatograms illustrating the second purification step for fractions PaE and PaF as described in 'Methods'. A stepwise gradient for fraction PaE, from 50 – 70% over 15 min, then from 70 – 100% over 10 min of solvent D (ammonium acetate 1 M) was used and allowed the separation of five fractions. Activity against Kv4.3 channels was recovered in PaE5. The other active fraction PaF4 was purified from the fraction PaF with a linear gradient from 50 – 100% solvent D over 25 min. The effluent was monitored at 280 nm. (D, E) The fractions PaE5 and PaF4 were further purified on C18 reverse phase column with a linear solvent B gradient from 10 – 50% over 40 min.


**Figure 2** PaTx1 and PaTx2 sequences. Homologies of phrixotoxins PaTx1 and PaTx2 with heteropodatoxins (HpTx1, HpTx2, and HpTx3) (Sanguinetti *et al*., 1997) from *Heteropoda venatoria* and with hanatoxins (HaTx1 and HaTx2) (Swartz & MacKinnon, 1997) from *Grammostola spatulata*. Black boxes indicate sequence identities, and grey boxes indicate sequence homologies.

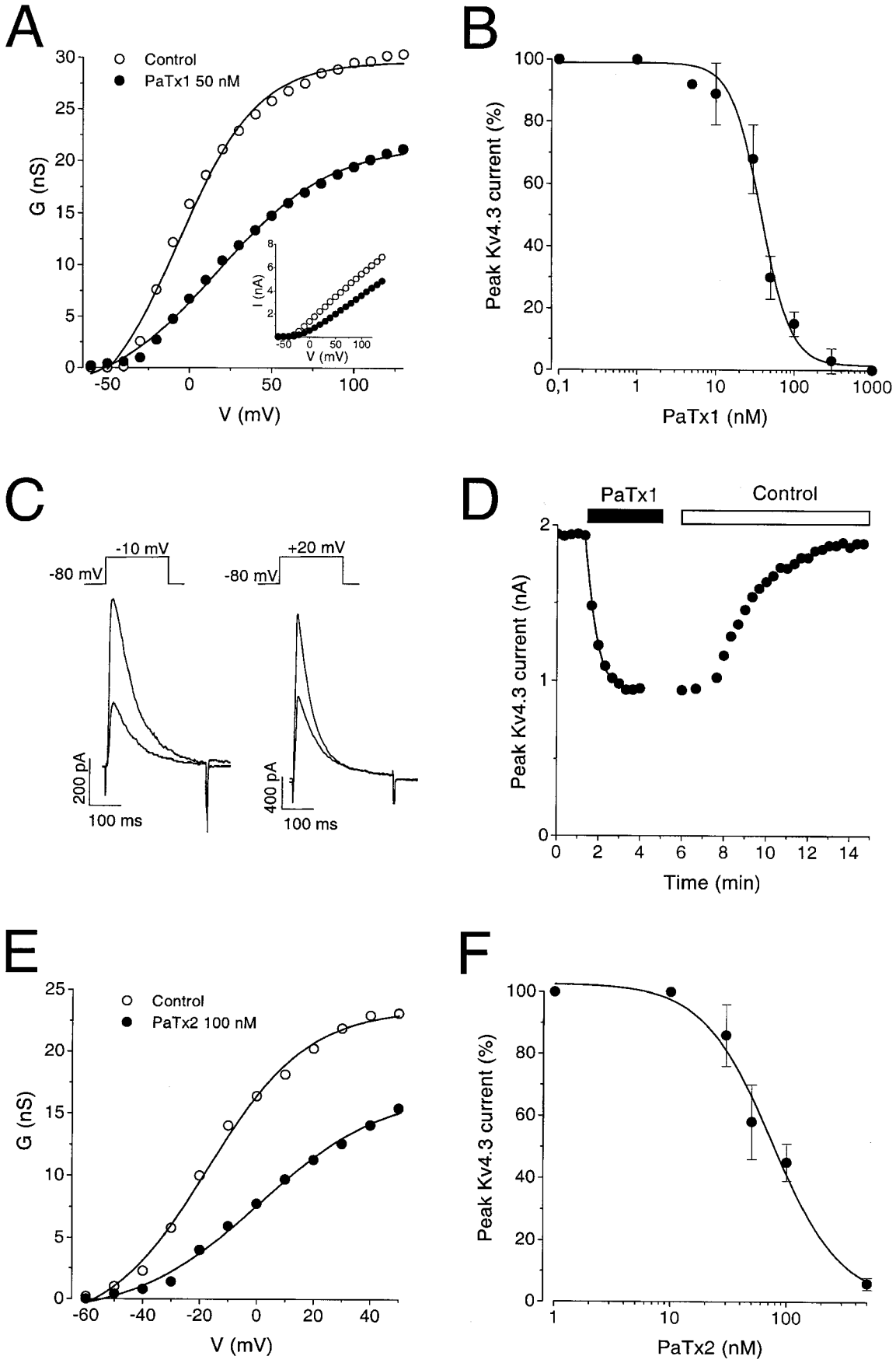


**Figure 3** Effect of PaTx1 and PaTx2 on Kv4.3 currents. Kv4.3 currents were recorded in COS transfected cells in the whole-cell configuration. Holding potential: −80 mV. (A) Conductance-voltage relationship for Kv4.3 peak current measured before and during application of 50 nM PaTx1. Conductances were calculated with equation (1): $G = I/(V - E_K)$ where G is the conductance, I the amplitude of the peak current, V the test potential, $E_K$ the reversal potential for $K^+$ (−85 mV). The $G_{max}$ value was evaluated from equation (2): $G = G_{max}/(1 + \exp(V_{0.5} - V)/k)$ where $V_{0.5}$ is the midpoint potential and k is the curve slope. In this example, the midpoint potential ($V_{0.5}$) values in control conditions and after inhibition by 50 nM PaTx1 were of −7 and +17 mV respectively. The $G_{max}$ values were 30 and 21 nS before and after PaTx1 inhibition. Inset: Current-voltage curve. Currents were induced by a set

**Table 1** Effects of PaTx1 on electrophysiological parameters of Kv4.2 and Kv4.3 channels

| | *Kv4.3* | | *Kv4.2* | |
|---|---|---|---|---|
| *Parameters* | *Control (test pulse in* mV*)* | *PaTx1 (concentration in* nM*)* | *Control (test pulse in* mV*)* | *PaTx1 (concentration in* nM*)* |
| Time to peak in ms ± s.e.mean<br>5 < n < 7 | 18 ± 2 (−10)<br><br>12 ± 1 (+20) | 22 ± 5 (50)<br>25 ± 4 (100)<br>14 ± 2 (50)<br>19 ± 2 (100) | 12 ± 1 (−10)<br><br>8 ± 1 (+20) | 23 ± 6 (30)<br>32 ± 4 (100)<br>14 ± 2 (30)<br>16 ± 2 (100) |
| $V_{0.5}$ act. in ms ± s.e.mean<br>2 < n < 9 | −5.6 ± 3 | +21 ± 3 (50)<br>+27 ± 3 (100) | −13 ± 2 | +11 ± 2 (50)<br>+25 ± 4 (100) |
| $V_{0.5}$ inact. in ms ± s.e.mean<br>2 < n < 10 | −61 ± 3 | −45 ± 5 (30) | −65 ± 2 | −52 ± 4 (30) |
| $\tau_i$ in ms ± s.e.mean<br>5 < n < 11 | 47 ± 6 (−10)<br>30 ± 5 (+20) | 75 ± 10 (100)<br>52 ± 9 (100) | 24 ± 5 (−10)<br>16 ± 3 (+20) | 55 ± 16 (30)<br>26 ± 6 (30) |
| $\tau_i$ in ms ± s.e.mean<br>3 < n < 8 | 194 ± 29 | 200 ± 45 (30) | 165 ± 32 | 165 ± 29 (10) |

Mean values ± s.e.mean are indicated for the corresponding parameters: $V_{0.5}$ act. is the midpoint potential calculated from equation (2) for the conductance-voltage relation. $V_{0.5}$ inact. is the midpoint potential given by the steady-state inactivation curve. $\tau_i$ is the time constant of inactivation of the Kv4 current evaluated from equation (4). $\tau_r$ is the time constant of recovery from inactivation for Kv4 currents calculated from equation (5).

### *Measurements of QT interval*

Bipolar electrodes were connected to an adjustable bandpass differential amplifier (ORTEC Inc., U.S.A.). The ECG channels were amplified and filtered between 1 and 100 Hz, and a stable signal was reliably obtained before we proceeded. Signals were collected, stored and analysed on a PC computer using PCLAMP software. The PR interval was measured from the beginning of the surface P wave to the beginning of the R wave complex. The QRS was measured from the beginning of the Q wave, when it was present, or from the base of the R to the bottom of the S wave. The QT interval is calculated from the beginning of the Q wave (or from the base of the R wave if not possible) to the end of the T wave, defined as the point at which it returns to the isoelectric baseline. Due to the early activation and fast inactivation of $I_{to1}$ *in vitro*, and in order to get a more specific measurement of the early phase of cardiac repolarization in mice, measurements were also made from the beginning of the S wave to the highest deflection of the rapid component of the T wave ($ST_{max}$) and to 50% of the steep descending slope of the rapid T wave (called $ST_r$ for 'ST rapid'). QT intervals were corrected with Bazett's formula ($Qtc(ms) = QT/RR(s)^{1/2}$) which allows comparisons of QT durations at different heart rates. For each mouse, a set of 10 cardiac cycle length-QT interval pairs was obtained from their ECG recordings.

### *Injection of PaTx1*

After recording of control parameters, 0.1–40 nmol of PaTx1 dissolved in 100 $\mu$l of saline were injected (<3 s) into a tail vein. ECGs were continuously recorded throughout the experiments up to 30 min after the injection.

### *Statistical analysis*

Results are shown as means ± s.e.mean. Continuous variables, as $QT_c$ and $ST_r$ values and their increase from baseline were analysed with a one way analysis of variance (ANOVA, Statview 4.5, and SuperAnova 1.11, Abacus Corp) or with a Mann-Whitney-Wilcoxon rank-sum test. $P<0.05$ was considered statistically significant.

## Results

### *Purification of two peptides active on Kv4 channels*

*P. auratus* whole venom fractionation on C18 reverse phase HPLC column yielded 10 fractions (noted A–J, see Figure 1A). The peaks PaE and PaF were selected for their blocking effects on Kv4.3 currents expressed in *Xenopus* oocytes and were further purified by an ion exchange purification step followed by a C18 reverse phase step (Figure 1B–E). Pure PaE5 and PaF4 peptides were eluted at 34 and 38% of acetonitrile respectively. The nomenclature that we propose for these toxins is phrixotoxin 1 (PaTx1) for PaE5 and phrixotoxin 2 (PaTx2) for PaF4.

PaTx1 has a molecular weight of 3547.60 Da and its sequence comprises 29 amino acids. It is 83.3% identical to PaTx2 (Figure 2). PaTx2, the most abundant peptide in the venom, has a

of depolarizing pulses at −60 to +120 mV in 10 mV increments. (B) Concentration-response relationship for PaTx1 block of the Kv4.3 current at −10 mV. The $IC_{50}$ value is 28 nM. The effects of 0.1 nM to 1 $\mu$M phrixotoxin on Kv4.3 currents were tested at −10 mV from a holding potential of −80 mV. The dose response curve was fitted by equation (3): $I = I_{max} + (I_{min} - I_{max})/(1 + \exp(C - IC_{50})/k))$ where I is the amplitude of the peak current, $I_{max}$ and $I_{min}$ are the amplitudes of the current corresponding to control and saturating concentrations of phrixotoxins respectively, C is the concentration of the toxin, $IC_{50}$ is the concentration of toxin which correspond to 50% $I_{max}$ and k is the curve slope. Each point is the mean ± s.e.mean of data from 3–6 cells. (C) Effect of 50 nM PaTx1 on Kv4.3 currents, recorded at a test pulse of −10 and +20 mV respectively, on the same cell. More blockade of Kv4.3 current by PaTx1 occurred at −10 mV (62%) than at 20 mV (51%). (D) Time course for Kv4.3 peak-current block with 50 nM PaTx1 at +20 mV and reversibility. The kinetics of current inhibition were fitted with equation (4): $I = I_{res} + I_{max}\exp(-t/\tau_i)$ where I is the amplitude of the peak current relative to time (t), $I_{max}$ is the initial peak current, $I_{res}$ is the non inactivating component and $\tau_i$ is the time constant of inhibition. $\tau_i$ value is 0.57 ms. (E) Conductance-voltage relationship for Kv4.3 peak current measured before and during application of 100 nM PaTx2. (F) Concentration-response relationship for PaTx2 block of the Kv4.3 current at −10 mV. Each point is the mean ± s.e.mean of data from 3–5 cells. The $IC_{50}$ value determined from equation (3) is 71 nM.

molecular weight of 3921.77 Da as revealed by EIMS and is composed of 31 amino acids with six cysteine residues. The molecular weights deduced from sequence determination for C-terminal amidated peptides are comparable to the EIMS values: 3548.41 Da for PaTx1 and 3921.67 Da for PaTx2.

PaTx1 and PaTx2 share 50 and 47% sequence identities with HpTx2, a spider toxin isolated from *Heteropoda venatoria* venom which also has a blocking activity on Kv4.2 channels (Sanguinetti *et al*., 1997). Only 20% sequence identities were found, however, with hanatoxins isolated from the spider *Grammostola spatulata*, and which are active on Kv2.1 and Kv4.2 channels (Swartz & McKinnon, 1997) (Figure 2). No sequence homologies were found with other known $K^+$ channel blockers.

### *Effects of PaTx1 and PaTx2 on Kv4.3 currents*

PaTx1 at a concentration of 50 nM significantly blocked the Kv4.3 currents elicited in COS cells ($70 \pm 7\%$ at $-10$ mV and $58 \pm 7\%$ at $+20$ mV, $n=5$ cells), (Figure 3A inset and C). Conductance-voltage relations showed that this inhibition results from a shift of the activation curve (Figure 3A). The dose-response curve of Kv4.3 current inhibition by PaTx1 at $-10$ mV yielded an $IC_{50}$ value of 28 nM (Figure 3B). The time course of the inhibition at $+20$ mV was best fitted, by a single exponential function with a time constant of 0.57 ms (Figure 3D). PaTx2 blocked Kv4.3 currents similarly but with a lower affinity ($IC_{50}=71$ nM, Figure 3E,F). Inhibition of Kv4.3 channels by PaTx1 or PaTx2 almost totally reversed

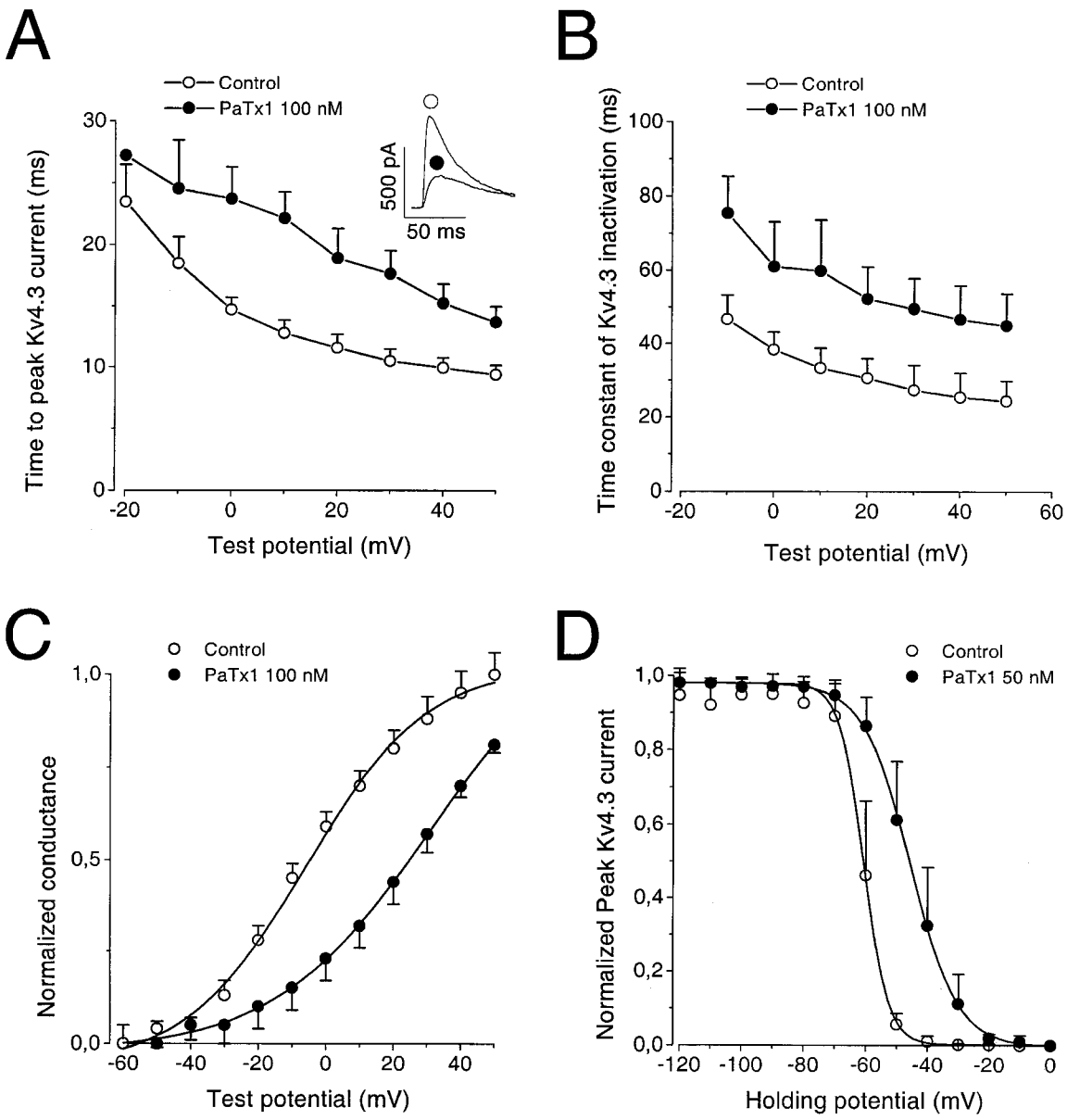


**Figure 4** Effects of PaTx1 on the kinetics of activation and inactivation of Kv4.3 currents. Kv4.3 currents were all recorded in COS transfected cells in the whole cell configuration. The holding potential is $-80$ mV. (A) The time-to-peak current is represented against the test potential for Kv4.3 channel before and after inhibition of the current by 100 nM PaTx1. The inset shows the effect of PaTx1 at $+20$ mV. (B) The time constant of current inactivation is plotted against the test potential for Kv4.3 channel before and after inhibition of the current by 100 nM PaTx1. The decay of current inactivation was fitted according to equation (4). (C) Normalized conductance-voltage relationships for Kv4.3 currents in control and after inhibition by 100 nM PaTx1. Relative conductances were obtained after normalization with the $G_{max}$ value. Points are means $\pm$ s.e.mean of data from four cells. (D) Steady-state inactivation curves for Kv4.3 currents evoked at $+30$ mV before and after their inhibition by 50 nM PaTx1. 10 s conditioning prepulses from $-120$ to $+10$ mV were applied prior to 200 ms depolarizing pulses to $+30$ mV. The same protocol was used after inhibition of Kv4.3 currents by PaTx1 at a concentration of 50 nM. The steady-state inactivation curves were fitted according to equation (3). Each point is the mean after normalization of Kv4.3 peak current amplitude from six cells.

upon washout (91±9% recovery after 5 min; $n=13$, Figure 3D).

### *PaTx1 changes Kv4.3 kinetics of activation and inactivation*

Mean values resulting from analysis of kinetic parameters are given in Table 1. The inhibition of Kv4.3 currents by PaTx1 (100 nM) is characterized by a concentration-dependent increase of the time-to-peak current (Figure 4A, Table 1). The Kv4.3 current inactivation is well fitted to a single exponential characterized by a time constant ($\tau_i$) which significantly increases in the presence of 100 nM PaTx1 (Figure 4B, Table 1). Inhibition of Kv4.3 currents by PaTx1 also induced a shift of the normalized conductance-voltage relation and of the voltage-dependence of steady-state inactivation to more depolarized potentials (Figure 4C,D, Table 1).

### *Recovery of Kv4.3 channel from inactivation*

At least 700 ms were required for Kv4.3 channels to recover from inactivation at −80 mV (Figure 5A,B). In control conditions, the Kv4.3 channel time constant for recovery ($\tau_r$) was not significantly modified by 30 nM of PaTx1 (Figure 5B, Table 1).

### *Voltage dependence of inhibition of Kv4.3 channels by PaTx1 toxin*

In order to determine the voltage dependence of Kv4.3 inhibition by PaTx1, high depolarizations (+130 mV) and/or pulse frequencies (0.2 and 1 Hz) were applied.

In 5 out of 8 cells, the current measured at +130 mV was inhibited by PaTx1 (29±2%) suggesting that the toxin was still bound to the channel, even at high depolarizations (Figure 5C,D).

The frequency of stimulation did not affect the affinity of PaTx1 for the Kv4.3 channels. After steady-state inhibition of the Kv4.3 currents at 0.2 Hz by PaTx1 (50 nM), the blockade was not modified by increasing the stimulation frequency to 1 Hz ($n=4$, data not shown). The steady-state inhibition of Kv4.3 currents was reached within 1.5 min whether at 0.2 or 1 Hz ($n=5$).

### *Preferential affinity of PaTx1 for the inactivated and resting closed states of Kv4.3 channels*

Affinity to the resting or inactivated states of the channel were evaluated by applying 50 nM of PaTx1 for 2 min prior to the first depolarization from either −80 or −40 mV up to −10 mV. Kv4.3 currents were equally inhibited in each of these conditions (Figure 5E,F). Inhibition was of 88±12% and 80±13%, $n=5$ and 4 cells) for the resting closed state and the inactivated state respectively as compared to inhibition obtained when PaTx1 was applied during the depolarizing step.

### *Effect of PaTx1 and PaTx2 on Kv4.2 currents*

PaTx1 (50 nM) potently blocked Kv4.2 currents (76±6% at −10 mV and 59±7% at +20 mV, $n=6$ cells), (Figure 6A). The toxin blocked Kv4.2 currents with more affinity ($IC_{50}=5$ nM) than the Kv4.3 currents evoked at −10 mV ($IC_{50}=28$ nM, Figure 6A). When fitted by a single exponential function, the time course of inhibition yielded a time constant of 0.53 ms (data not shown).

PaTx2 similarly blocked the Kv4.2 currents but with a lower affinity ($IC_{50}=34$ nM, not shown). PaTx1 or PaTx2 inhibition of the Kv4.2 channels almost totally reversed upon washout (89±9% recovery after 5 min; $n=10$ cells).

### *Characteristics of Kv4.2 channel inhibition by PaTx1*

PaTx1-induced modifications of the Kv4.2 electrophysiological parameters were comparable to those observed on Kv4.3 channels (see Table 1). PaTx1 decreased dose-dependently the kinetics of activation of the Kv4.2 current (Figure 6C). The time constants of Kv4.2 current inactivation were increased by 30 nM PaTx1 (Figure 6D). A shift of the normalized conductance-voltage and of the steady-state inactivation curves to more depolarized potentials occurred during application of 30 nM PaTx1 (Figure 6E,F). The time constant for recovery of the Kv4.2 channels ($\tau_r$) was not modified by 10 nM of PaTx1 (Table 1).

The change of the stimulation frequency had no effect on the affinity and the kinetics of inhibition of PaTx1 for the Kv4.2 channel. After reaching steady-state block at 0.2 Hz, a stimulation frequency of 1 Hz did not modify the inhibition exerted by 30 nM PaTx1 ($n=4$). The time required to reach steady-state inhibition was 1.5 min in both cases (data not shown).

PaTx1 blocked Kv4.2 channels in the closed and inactivated states. Kv4.2 currents evoked by depolarizations to −10 mV were similarly blocked by a 2 min application of 30 nM of PaTx1, either at −80 or −40 mV, as compared to the blockade obtained by applying the toxin during the depolarizing pulses (relative inhibition: 88±9% and 81±13%, respectively, data not shown).

### *Effect of PaTx1 on $I_{to1}$ current in cardiomyocytes*

In a preliminary study, PaTx1 (50 nM) significantly blocked the $I_{to1}$ current (by 60±7%, $n=5$) evoked from depolarizations to +20 mV from a holding potential of −80 mV in isolated rat cardiomyocytes.

### *Effect of PaTx1 and PaTx2 on Kv4.1 currents*

Kv4.1 currents expressed in COS cells were resistant to PaTx1 and PaTx2 block: 250 nM PaTx1 only blocked 39±4% ($n=4$ cells) and 300 nM PaTx2 blocked 20±2% of the Kv4.1 currents evoked at −10 mV.

### *Specificity of phrixotoxins on the Kv4 subfamily of channels*

Specificity of PaTx1 and PaTx2 toxins for Kv4 channels was evaluated by applying the toxins on different cloned $K^+$ channels expressed either in the *Xenopus* oocytes or in COS transfected cells. None of the Kv1 channel family recorded in *Xenopus* oocytes (Kv1.1, Kv1.2, Kv1.3, Kv1.4, Kv1.5) were sensitive to up to 5 μM of PaTx1 or PaTx2 (data not shown). Furthermore, neither HERG, that underlies the cardiac rapid component $I_{Kr}$ of the delayed rectifier $I_K$ (Attali, 1996; Sanguinetti *et al.*, 1995), nor the human KvLQT1 channel coexpressed with IsK that composes its slow component $I_{Ks}$, were affected by up to 0.3 μM PaTx1 when recorded in transfected COS cells (Barhanin *et al.*, 1996).

The 20% sequence identity that PaTx1 and PaTx2 share with hanatoxins which are active on Kv2.1 channels (Swartz & McKinnon, 1997) prompted us to test the phrixotoxins on

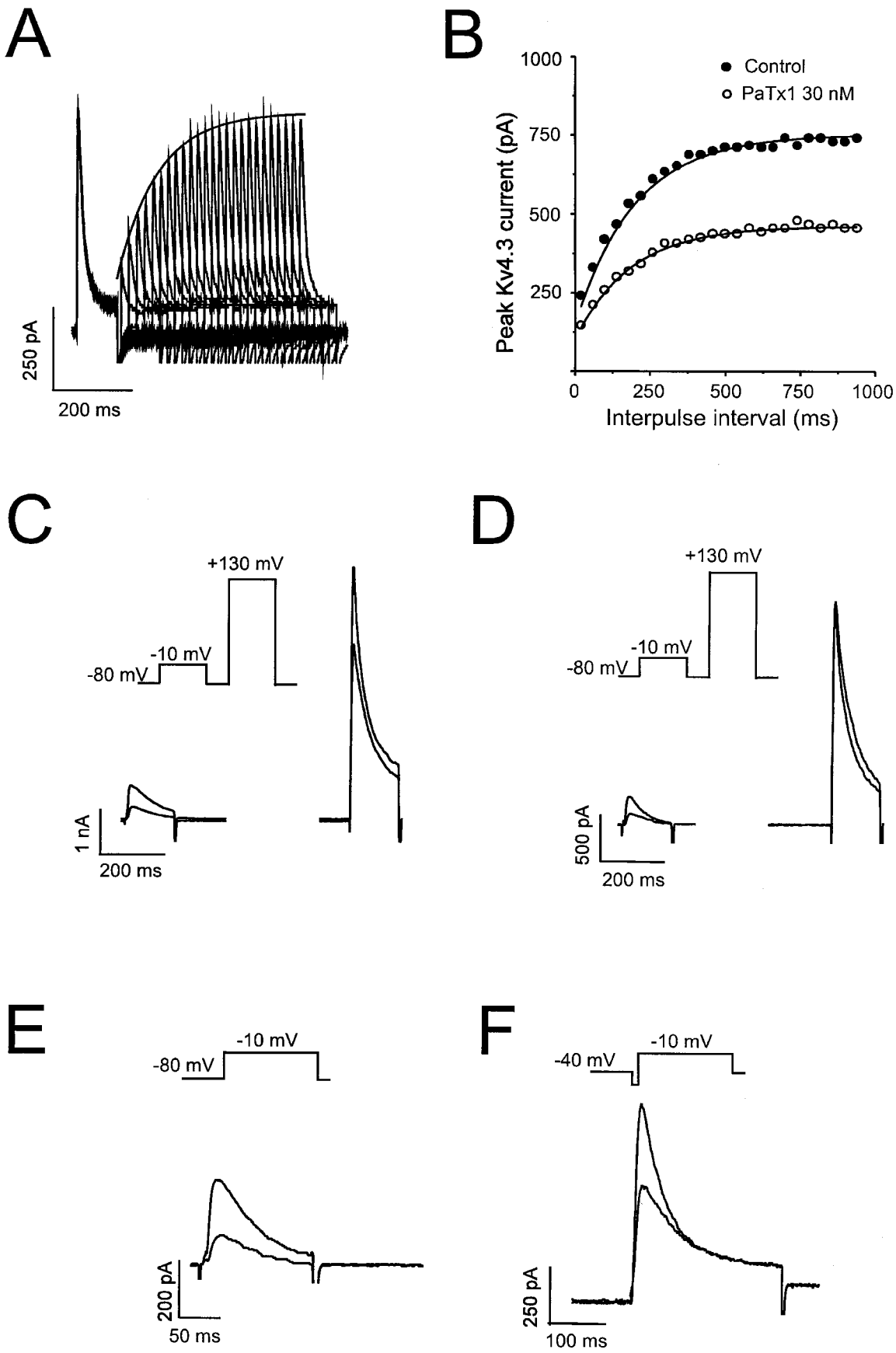


**Figure 5** Voltage dependent inhibition of Kv4.3 channels by PaTx1. Kv4 currents were recorded in COS transfected cells in the whole-cell configuration. The holding potential was −80 mV. (A) Successive traces illustrating recovery from Kv4.3 channel inactivation in control conditions. The corresponding fit for the peak Kv4.3 current evoked at +10 mV is superimposed with the traces. (B) Peaks Kv4.3 currents were plotted against the interpulse interval in control and after inhibition by 30 nM of PaTx1. The time constant for recovery from channel inactivation was determined using a double pulse protocol where cells were depolarized from −80 mV to +10 mV for 200 ms with increasing interpulse intervals of time at −80 mV (dt = 20 ms). Peak currents elicited by depolarizing pulses were plotted as a function of time and data points were fitted to equation (5): $I = I_{res} + I_{max}(1 - \exp - t/\tau_r)$ where I is the peak current elicited by the second pulse, $I_{max}$ is the amplitude of peak current elicited by the test pulse after recovery at

Kv2.1 and Kv2.2 currents. The Kv2.1 and Kv2.2 currents evoked at +20 mV from a holding potential of −80 mV were resistant to either 0.5 μM PaTx1 (inhibition of Kv2.1: 6±3%, $n=5$ and Kv2.2: 16±10%, $n=8$) or 0.5 μM PaTx2 (inhibition of Kv2.1: 8±5%, $n=4$ and Kv2.2: 11±6%, $n=5$).

None of the cloned channels from the Kv3 family recorded in injected *Xenopus* oocytes (Kv3.1, Kv3.2 and Kv3.4), were sensitive to phrixotoxins (up to 1 μM, $n=3$ for each channel).

The inward rectifier channel IRK1 expressed in *Xenopus* oocytes was also insensitive to 1 μM PaTx1 or PaTx2, as was the recently cloned two P domain background $K^+$ channel TREK-1 (Fink *et al*., 1996; Patel *et al*., 1998), expressed in COS cells.

PaTx1 and PaTx2 toxins weakly blocked the neuronal TTX-sensitive $Na^+$ currents of neuroblastoma cells but only at relatively high concentrations (13±8% inhibition by 0.1 μM PaTx1, $n=5$ and 14±5% inhibition by 0.5 μM PaTx2, $n=2$).

These results indicate that PaTx1 and PaTx2 are good blockers of the Kv4 channel family with a marked specificity towards Kv4.2 and Kv4.3 channels.

### *Electrocardiographic modifications of cardiac repolarization induced by intravenous injections of PaTx1 in anaesthetized mice*

Three bipolar lead electrocardiograms (ECGs, DI, DII, DIII) were recorded under pentobarbital anaesthesia before, during and after toxin injection with a good stability of the signal from all 11 mice studied (Figure 7). P wave, PR, QRS, $ST_{max}$, $ST_r$ and QT intervals could be reliably measured in all animals. The average cycle length (RR interval) was 159±14 ms. The P wave duration was 19±2 ms, the PR interval was 36.5±2.1 ms and the QRS interval was 12.1±0.5 ms (Figure 7A). The T wave was biphasic with a rapid component, and a slower one either positive or negative to the isoelectric line. The duration of the $ST_{max}$ interval was 4.20±0.62 ms, and the $ST_r$ interval 9.25±0.89 ms. The average QT duration on the first recording of the experiment was 100±9 ms, which corresponded to a QTc interval of 249±11 ms. The injection of concentrations of PaTx1, ranging from 0.1–40 nmol, did not change significantly the RR interval, from 159±14 ms in control conditions to 166±10 ms after the injection ($P=0.15$, N.S.). The PR interval (39.2±2.3 ms) did increase in some mice (Figure 8A) whereas the QRS interval duration (12.2±0.4 ms) did not significantly change from control values, excluding therefore a relevant effect of the toxin on $Na^+$ and/or $Ca^{2+}$ currents. However, PaTx1 significantly increased the mean duration of the ventricular repolarization ($QT_c$) from 249±11 to 265±8 ms ($n=10$, $P<0.05$). The toxin effects were mainly observed on the fast component of the T wave, which amplitude significantly decreased and which duration significantly increased after the toxin injection (Figure 7B). Thus, $ST_{max}$ values increased from 4.20±0.62 to 5.00±0.72 ms, which represents an increase of 22±6% ($P<0.05$, $n=10$), and $ST_r$ from 9.25±0.89 to 11.21±0.99 ms, representing an increase of 22±4% ($P<0.01$, $n=10$). There was a clear dose-effect relationship between the toxin injected and the resulting modifications of the fast T wave parameters ($ST_{50}$, Figure 8C). Besides those ECG effects, a generalized vasoconstriction was noticed after PaTx1 injection, followed by various transient cardiac rhythm and/or conduction problems including second and third degree atrio-ventricular (AV) block (4 out of 11 mice, Figure 8B), premature ventricular beats (Figure 7) and ventricular tachycardia (3 out of 11 mice).

## Discussion

Voltage-gated potassium channels have a key role in controlling the rate of repolarization of neuronal and cardiac cells of excitable tissues. The members of the Kv4 subfamily are characterized by rapidly activated and inactivated currents. It is believed that *Shal* related Kv4 proteins are key components of the classical A-type $K^+$ channels underlying the A-currents ($I_A$) found in many neuronal soma. A-type $K^+$ channels are of particular interest because of their roles in regulating firing frequency, spike initiation and waveform. Three members have been identified in this $K^+$ channel family, Kv4.1, Kv4.2 and Kv4.3. Kv4.1 is expressed at low levels in the brain, while Kv4.2 and Kv4.3 transcripts appear to be abundant, each with a unique pattern of expression, although there is an overlap expression of Kv4.2 and Kv4.3 transcripts in several neuronal regions (Serodio & Rudy, 1998; Serodio *et al*., 1996) suggesting the possible formation of heteropolymeric channels.

Further analyses of the precise physiological role of $I_{to1}$ require specific and high affinity blockers. The two new toxins identified in this work, PaTx1 and PaTx2, are both specific and potent inhibitors of Kv4.2 and Kv4.3 channels. Concentrations of 100 nM of either PaTx1 or PaTx2 almost completely block both Kv4.3 and Kv4.2 currents while they are without effect on the Kv4.1 channel. The toxins alter the gating of the channels, by changing both their activation and inactivation properties. Phrixotoxins bind to Kv4.2 and Kv4.3 channels with a high affinity at both closed and inactivated states and display no use- or reverse-use-dependence. Both toxins induce a blockade that is maximal in a low depolarization range but

−80 mV for 20 s. $I_{res}$ is the amplitude of the residual current remaining at the end of the first pulse, t the interval of time between the first and the second test pulses at +10 mV and $\tau_r$ the time constant of recovery. PaTx1 was tested at a concentration of 30 nM on the Kv4.3 current in order to block at least 50% of the current. Fit curves are shown and corresponding values for $\tau_r$ are: 199 ms in control and 185 ms after PaTx1 inhibition. (C) Effect of 50 nM PaTx1 on Kv4.3 current at high depolarizations to +130 mV. To test whether PaTx1 was still bound to the channel after large depolarizations, a test pulse to +130 mV was applied 700 ms after a 150 ms depolarization to −10 mV from a holding potential of −80 mV, in the absence (control) and in the presence of the toxin. In this example, the Kv4.3 current is inhibited by PaTx1 at −10 mV by 60% and at +130 mV by 18%. (D) In another example, using the same protocol as in (C), the Kv4.3 current is inhibited by PaTx1 at −10 mV by 63% and not at all at +130 mV. (E) PaTx1 is able to block the Kv4.3 channel in a closed state. The membrane potential was maintained at −80 mV during 2 min in the presence of a concentration of PaTx1 (50 nM), known to block 70% of the Kv4.3 current, before applying a depolarizing pulse to −10 mV. The inhibition of the current was measured after applying the toxin for 2 min to obtain the steady-state inhibition. Under a 2 min perfusion of 50 nM of PaTx1 at −80 mV, the Kv4.3 current is inhibited by 60% as early as the first stimulation to −10 mV. (F) PaTx1 can block the Kv4.3 channel in an inactivated state. The interaction of the toxin with the inactivated state of the channel was tested using a membrane potential maintained at −40 mV. After 2 min of superfusion with 50 nM PaTx1, the membrane potential was clamped to −80 mV during 700 ms for recovery from inactivation, followed by a depolarizing pulse to −10 mV. Comparison to control values assessed the degree of blockade. Under a 2 min perfusion of 50 nM of PaTx1 at −40 mV, the Kv4.3 current was inhibited by 70% as early as the first stimulation to −10 mV.

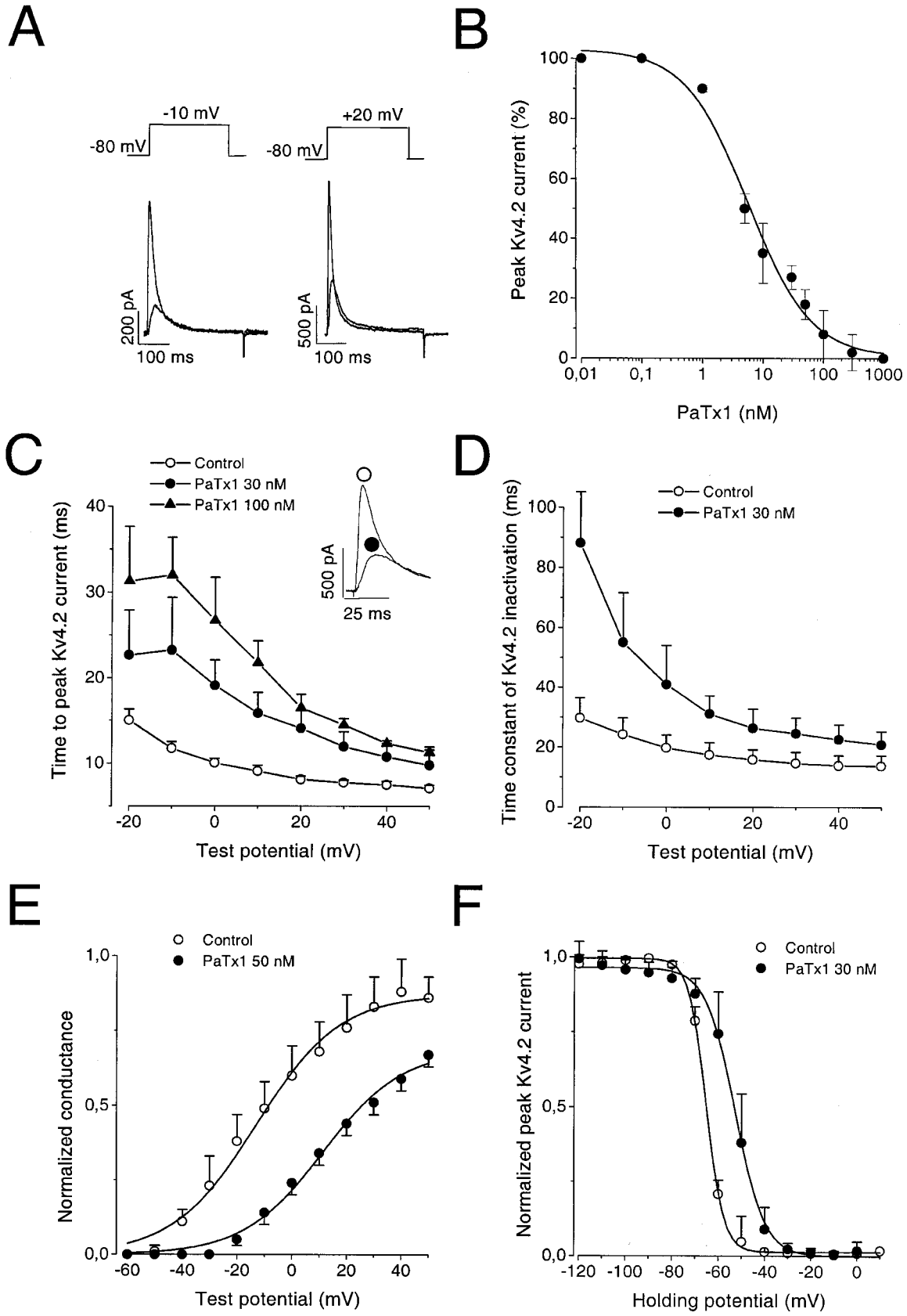


**Figure 6** Effect of PaTx1 and PaTx2 on Kv4.2 currents. Kv4.2 currents were recorded in COS transfected cells in the whole-cell configuration. Holding potential: −80 mV. (A) Effect of 50 nM PaTx1 on Kv4.2 currents, recorded at a test pulse of −10 mV and +20 mV respectively, on the same cell. More blockade of Kv4.2 current by PaTx1 occurred at −10 mV (79%) than at +20 mV (67%). (B) Concentration-response relationship for PaTx1 block of the Kv4.2 current at −10 mV. Each point is the mean ± s.e.mean of data from 3–7 cells. The $IC_{50}$ value determined from equation (3) is 5 nM. (C) The time-to-peak current is represented against the test potential for Kv4.2 channel before and after inhibition of the current by 30 and 100 nM PaTx1. The inset shows the effect of 30 nM PaTx1 at 20 mV. (D) The time constant of current inactivation is plotted against the test potential for Kv4.2 channel before and after inhibition of the current by 30 nM PaTx1. (E) Normalized conductance-voltage relationships for Kv4.2 currents in control and after inhibiton by 50 nM PaTx1. Points are means ± s.e.mean of data from three cells. (F) Steady-state inactivation curves for Kv4.2 currents evoked at +30 mV before and after their inhibition by 30 nM PaTx1. Each point is the mean after normalization of Kv4.2 peak current amplitude from 7–9 cells.

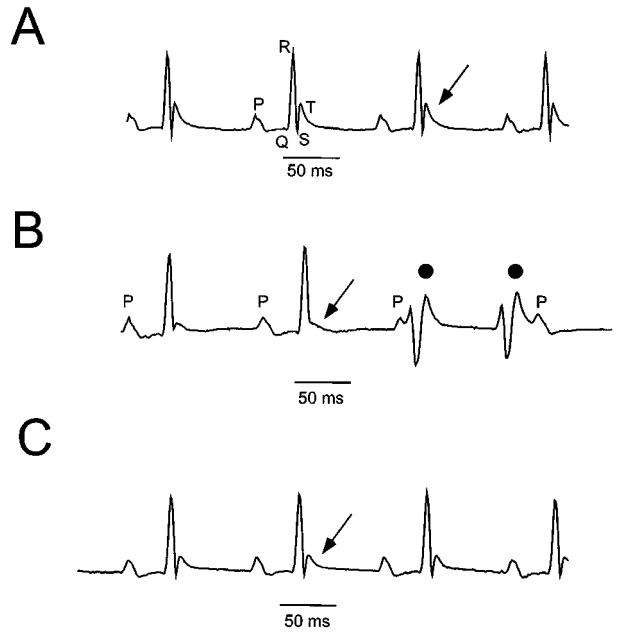


**Figure 7** Electrocardiographic modifications induced by intravenous injections of PaTx1 in mice. (A) A representative lead I surface control ECG, recorded from a Balb C female by Pclamp Software (Axon). P, Q, R and T describe the P wave (atrial depolarization), the PR interval (atrio-ventricular conduction), QRS wave (ventricular depolarization) and the biphasic T wave (ventricular repolarization). The cycle length (RR) on the upper trace is 130 ms, with a PR at 37.5 ms, and QT at 62 ms. (B) ECG recorded 3 min after the intravenous injection of 12 nmol of PaTx1. The QT interval increased to 71 ms. A significant decrease of the fast component of the T wave occurred (arrow) and typical premature ventricular beats appeared (●). (C) The T wave modifications progressively reversed 20 min after the injection of PaTx1.

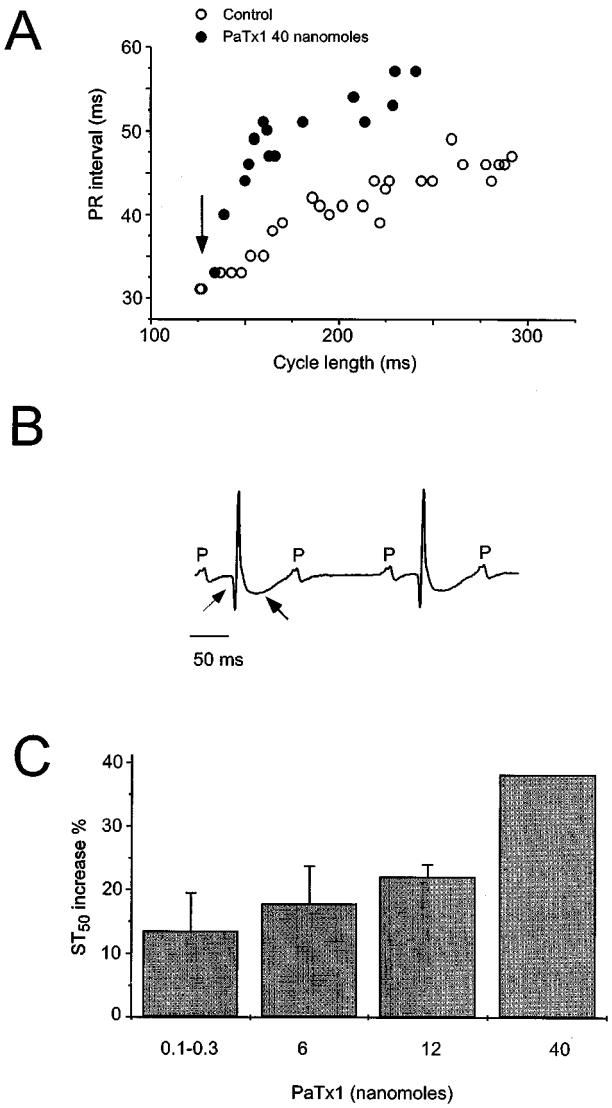


**Figure 8** Electrocardiographic modifications induced by high concentrations of PaTx1 in mice. (A) Plot of the PR-RR relationships in a representative mouse, obtained during two successive anaesthesia, in control conditions and after injecting of 40 nmol of PaTx1. After anaesthesia induction, the heart rate progressively decrease, and the PR interval was prolonged accordingly, reflecting the AV conduction. Within seconds after the intravenous injection of PaTx1 (arrow), the PR interval abruptly increased. (B) A typical second degree atrio-ventricular block occurred 2 min after the injection of 40 nmol of PaTx1 with myocardial infarction. Note the Q wave and the huge negative T wave (arrows). (C), Dose-effect relationship of PaTx1 and the resulting increase in $ST_{50}$ measured 5 min after the injection ($n = 11$).

wanes and remains incomplete at high depolarizations. The fact that large depolarizations (+130 mV) can overcome the blocking effect is not uncommon for spider toxins. Such a phenomenon has already been described for the effects of hanatoxins on Kv2.1 channels (Swartz & McKinnon, 1997) and heteropodatoxins (HpTx) on Kv4.2 channels (Sanguinetti *et al*., 1997) The ~50% identity that PaTx1 and PaTx2 share with HpTx2 and the fact that the location pattern of the cysteine residues is conserved among their subgroup, suggest a similar mode of action, even though these toxins are extracted from venoms from different spider families (Heteropodidae for HpTx and Theraphosidae for PaTx). However, besides blocking Kv4.2 channels, PaTx1 and PaTx2 also strongly inhibit the Kv4.3 channels, a property which had not been investigated for HpTx. On the other hand, it is not known whether HpTx inhibit $K^+$ channels such as Kv1.1, Kv1.2, Kv1.3, Kv1.5, or of the Kv3 family, or of the inward rectifier and background $K^+$ channel families.

Because of the abundant presence of Kv4 channels in the nervous system, it is not surprising that neurological effects were observed after intravenous injection of PaTx1 in mice. They were mainly characterized by a motor impairment prevailing on the posterior limbs and convulsions (data not shown). These effects are much less severe than those observed after intravenous injections of the MCD-peptide, a bee venom toxin, or of the dendrotoxins from the snake *Dendroaspis* venoms, which block the Kv1.1, Kv1.2 an Kv1.6 channels (Grissmer *et al*., 1994; Halliwell *et al*., 1986; Pongs, 1992b; Schweitz, 1984; Strong, 1990), inducing very severe epileptic seizures and convulsions (Bagetta *et al*., 1992; Mourre *et al*., 1997). The neurotoxic effects of PaTx1 were similar whether the toxin injection was intravenous or intracisternal (data not shown), making it likely that PaTx1 crosses the blood brain barrier at least to some extent despite its peptidic nature.

There is an increasing body of evidence, including antisense and transgenic experiments (Johns *et al*., 1997; Nakamura *et al*., 1997) suggesting that Kv4.2 and Kv4.3 underlie the $I_{to1}$ current in cardiac cells (Serodio *et al*., 1996). First, Kv4.3 mRNA is expressed at significant levels in rat, canine and human cardiac myocytes eliciting rapidly inactivating A type potassium currents. Second, the kinetics and the current-voltage relationships of Kv4.2 and Kv4.3 channels closely resemble those of the native $I_{to1}$ current. Third, both Kv4.3, Kv4.2 and $I_{to1}$ share pharmacological similarities like insensitivity to the $K^+$ channel blocker TEA and inhibition

by 4-aminopyridine (4-AP) or the antiarrhythmic drug flecainide (Grissmer *et al*., 1994; Tseng *et al*., 1996; Yeola & Snyders, 1997). In addition, differential expressions of Kv4.2 and Kv4.3 in different heart regions, like their predominance in atria or their characteristic transmural ventricular gradient clearly correspond to differential expression of the $I_{to1}$ current explaining a faster repolarization in atria or in the subepicardial layers of the ventricle (Dixon & McKinnon, 1994; Dixon *et al*., 1996; Serodio & Rudy, 1998; Serodio *et al*., 1996; Yeola & Snyders, 1997).

The Kv1.5 gene which is highly expressed in the heart encodes $I_{Kur}$, the 4-AP sensitive sustained component of *Ito* (Guo *et al*., 1997; Po *et al*., 1993). The insensitivity of the Kv1.5 current to the phrixotoxins permits to discriminate the respective physiological roles of $I_{to1}$ and $I_{Kur}$. This is important in mice given the role of the fast repolarizing currents that enable heart rates to approximate 600 beats $min^{-1}$.

The intravenous injection of PaTx1 in mice resulted in various transient heart rhythm and conduction problems. Within seconds after the injection, mice experienced different degrees of AV block (from a sharp augmentation of the PR interval to higher degrees of AV block). This points to the role that the Kv4 subfamily of channels might play in the conductive system, whether in the AV node or in the His bundle. The fact that toxin injections could induce ventricular arrhythmia indicates that events resulting in $I_{to1}$ blockade (secondary effects of drugs, possible mutations in Kv4 channels) will generate these sorts of arrhythmia. $I_{to1}$ plays an important role in shaping the early phase of the cardiac action potential repolarization. ECG parameters show that intravenous injections of PaTx1 induce a dose-dependent decrease of the rapid component of the T wave and a prolongation of the QT interval. These effects on the T wave occur right after the QRS deflection, which corresponds to the rapid depolarization phase of the ventricular action potential where $I_{to1}$ is activated.

In conclusion, we have isolated and purified from the venom of *Phrixotrichus auratus* two new toxins, PaTx1 and PaTx2, that are potent and specific blockers of Kv4.2 and Kv4.3 channels. The use of these pharmacological tools has confirmed the view that Kv4.2 and Kv4.3 channels are the essential components of $I_{to1}$ current in cardiac cells. It has also contributed to the better understanding of the exact role of $I_{to1}$ in cardiac electrogenesis in a mouse model.

Other types of Kv channels such as Kv1.4 or Kv3.4 also generate rapidly inactivating A-type $K^+$ channels (Rettig *et al*., 1992; Tseng-Crank *et al*., 1990). No specific toxin has been found yet for the Kv1.4 channels. However, because phrixotoxins block Kv4.2 and Kv4.3 channels without affecting Kv1.4 channels, A-type channels resulting from Kv1.4 expression or from Kv4.2/Kv4.3 expressions can now be easily discriminated. Easy discrimination can also be made between relative contributions of Kv3.4, Kv4.2 and Kv4.3 channels, since sea anemone BDS toxins (but not phrixotoxins) selectively block the Kv3.4 channels (Diochot *et al*., 1998).

We gratefully thank Drs L. Salkoff, L. Jan and D. McKinnon for the generous gift of Kv4.1, Kv4.2 and Kv4.3 respectively. We thank Dr G. Romey for helpful discussions. This work was supported by the Centre Nationale de la Recherche Scientifique (C.N.R.S.), the Association Française contre les myopathies (A.F.M.), and the Ministère de la Défense Nationale (Grant DRET 96/096).

## References

AIYAR, J., WITHKA, J.M., RIZZI, J.P., SINGLETON, D.H., ANDREWS, G.C., LIN, W., BOYD, J., HANSON, D.C., SIMON, M., DETHLEFS, B., LEE, C., HALL, J.E., GUTMAN, G.A. & CHANDY, K.G. (1995). Topology of the pore-region of a $K^+$ channel revealed by the NMR-derived structures of scorpions toxins. *Neuron,* **15,** 1169–1181.

ATTALI, B. (1996). Ion channels A new wave for heart rhythms. *Nature,* **384,** 24–25.

BAGETTA, G., NISTICO, G. & DOLLY, J.O. (1992). Production of seizures and brain damage in rats by α-dendrotoxin, a selective $K^+$ channel blocker. *Neurosci. Lett.,* **139,** 24–40.

BALDWIN, T.J., TSAUR, M.-L., LOPEZ, G.A., JAN, Y.N. & JAN, L.Y. (1991). Characterization of a mammalian cDNA for an inactivating voltage-sensitive $K^+$ channel. *Neuron,* **7,** 471–483.

BARHANIN, J., LESAGE, F., GUILLEMARE, E., FINK, M., LAZDUNSKI, M. & ROMEY, G. (1996). KvLQT1 and Isk (minK) proteins associate to form the IKs cardiac potassium current. *Nature,* **384,** 78–80.

BARRY, D.M., TRIMMER, J.S., MERLIE, J.P. & NERBONNE, J.M. (1995). Differential expression of voltage-gated K channel subunits in adult rat heart. Relational to functional K channels? *Circ. Res.,* **77,** 361–369.

BARRY, D.N. & NERBONNE, J.M. (1996). Myocardial potassium channels: electrophysiological and molecular diversity. *Ann. Rev. Physiol.,* **58,** 363–394.

BIDARD, J.-N., MOURRE, C. & LAZDUNSKI, M. (1987). Two potent central convulsant peptides, a bee venom toxin, the MCD peptide, and a snake venom toxin, dendrotoxin I, known to block K channels, have interacting receptor sites. *Biochem. Biophys. Res. Commun.,* **143,** 383–389.

DIOCHOT, S., SCHWEITZ H., BERESS, L. & LAZDUNSKI, M. (1998). Sea anemone peptides with a specific blocking activity against the fast inactivating potassium channel Kv3.4. *J. Biol. Chem.,* **273,** 6744–6749.

DIXON, J.E. & MCKINNON, D. (1994). Quantitative analysis of potassium channel mRNA expression in atrial and ventricular muscle of rats. *Circ. Res.,* **75,** 252–260.

DIXON, J.E., SHI, W., WANG, H.-S., MCDONALD, C., YU, H., WYMORE, R.S., COHEN, I.S. & MCKINNON, D. (1996). Role of the Kv4.3 K channel in ventricular muscle: a molecular correlate for the transient outward current. *Circ. Res.,* **79,** 659–668.

DUPRAT, F., GUILLEMARE, E., ROMEY, G., FINK, M., LESAGE, F., LAZDUNSKI, M. & HONORE, E. (1995). Susceptibility of cloned K channels to reactive oxygen species. *Proc. Natl. Acad. Sci. U.S.A.,* **92,** 11796–11800.

FINK, M., DUPRAT, F., LESAGE, F., REYES, R., ROMEY, G., HEURTEAUX, C. & LAZDUNSKI, M. (1996). Cloning, functional expression and brain localisation of a novel unconventional outward rectifier K channel. *EMBO J.,* **15,** 6854–6862.

GARCIA, M.L., GARCIA-CALVO, M., HIDALGO, P., LEE, A. & MCKINNON, R. (1994). Purification and characterization of three inhibitors of voltage-dependent K channels from *Leiurus quinquestriatus* var. *hebraeus* venom. *Biochemistry,* **33,** 6834–6839.

GRISSMER, S., NGUYEN, A.N., AIYAR, J., HANSON, D.C., MATHER, R.J., GUTMAN, G.A., KARMILOWICZ, M.J., AUPERIN, D.D. & CHANDY, K.G. (1994). Pharmacological characterization of five cloned voltage-gated K channels, types Kv1.1, 1.2, 1.3, 1.5, and 3.1, stably expressed in mammalian cell lines. *Mol. Pharmacol.,* **45,** 1227–1234.

GUO, W., KAMIYA, K. & TOMOYA, J. (1997). Roles of the voltage-gated K channel subunits, Kv1.5 and Kv1.4, in the developmental changes of K currents in cultured neonatal rat ventricular cells. *Pflügers Arch.,* **434,** 206–208.

HALLIWELL, J.V., OTHMAN, I.B., PELCHEN-MATTHEWS, A. & DOLLY, J.O. (1986). Central action of dendrotoxin: selective reduction of a transient K conductance in hippocampus and binding to localized acceptors. *Proc. Natl. Acad. Sci. U.S.A.,* **83,** 493–497.

HARVEY, A.L. & ANDERSON, A.J. (1991). Dendrotoxins: snake toxins that block potassium channels and facilitate neurotransmitter release. In *Snake Toxins* ed. Harvey, A.L. pp. 131–164. New York: Pergamon Press Inc.

JOHNS, D.C., NUSS, H.B. & MARBAN, E. (1997). Suppression of neuronal and cardiac transient outward currents by viral gene transfer of a dominant negative Kv4.2 construct. *Biophys. J.,* **72,** A349.

JURMAN, M.E., BOLAND, L.M. & YELLEN, G. (1994). Visual identification of individual transfected cells for electrophysiology using antibody-coated beads. *Biotechniques,* **17,** 876–881.

KACZMAREK, L.K. & STRUMWASSER, F. (1984). A voltage clamp analysis of currents underlying cAMP-induced membrane modulation of isolated peptidergic neurons of Aplysia. *J. Neurophysiol.,* **52,** 340–349.

LITOVSKY, S. & ANTZELEVITCH, C. (1987). Transient outward current prominent in canine ventricular epicardium but not endocardium. *Circ. Res.,* **62,** 116–126.

MILLER, C. (1995). The charybdotoxin family of K channel-blocking peptides. *Neuron,* **15,** 5–10.

MITRA, R. & MORAD, M. (1986). A uniform enzymatic method for the dissociation of myocytes from heart and stomach of vertebrates. *Am. J. Physiol.,* **249,** H1056–H1060.

MOCKZYDLOWSKI, E., LUCCHESI, K. & RAVIDRAN, A. (1988). An emerging pharmacology of peptide toxins targeted against potassium channels. *J. Membr. Biol.,* **105,** 95–111.

MOURRE, C.M., LAZDUNSKI, M. & JARRARD, L.E. (1997). Behaviors and neurodegeneration induced by two blockers of K channels, the mast cell degranulating peptide and Dendrotoxin I. *Brain Res.,* **762,** 223–227.

NAKAMURA, T.Y., COETZEE, W.A., VEGA-SAENZ DE MIERA, E., ARTMAN, M. & RUDY, B. (1997). Modulation of Kv4 channels, key components of rat ventricular transient outward K current, by PKC. *Am. J. Physiol.,* **273,** H1775–H1786.

PAK, M.D., BAKER, K., COVARRUBIAS, M., BUTLER, A., RATCLIFFE, A. & SALKOFF, L. (1991). *mShal*, a subfamily of A-type K channel cloned from mammalian brain. *Proc. Natl. Acad. Sci. U.S.A.,* **88,** 4386–4390.

PATEL, A.J., HONORE, E., MAINGRET, F., LESAGE, F., FINK, M., DUPRAT, F. & LAZDUNSKI, M. (1998). A mammalian two pore domain mechano-gated S-type $K^+$ channel. *EMBO J.,* **17,** 4283–4290.

PO, S., ROBERDS, S., SNYDERS, D.J., TAMKUM, M.M. & BENNETT, P.B. (1993). Heteromultimeric assembly of human potassium channels. Molecular basis of a transient outward current? *Circ. Res.,* **72,** 1326–1336.

PONGS, O. (1992a). Molecular biology of voltage-dependent potassium channels. *Physiol. Rev.,* **72,** S69–S88.

PONGS, O. (1992b). Structural basis of voltage-gated K channel pharmacology. *Trends Physiol. Sci.,* **13,** 359–365.

REHM, H., BIDARD, J.-N., SCHWEITZ, H. & LAZDUNSKI, M. (1988). The receptor site for the bee venom mast cell degranulating peptide. Affinity labeling and evidence for a common molecular target for mast cell degranulating peptide and dendrotoxin I, a snake toxin active on K channels. *Biochemistry,* **27,** 1827–1832.

REHM, H. & LAZDUNSKI, M. (1988). Purification and subunit structure of a putative K-channel protein identified by its binding properties for dendrotoxin I. *Proc. Natl. Acad. Sci. U.S.A.,* **85,** 4919–4923.

RETTIG, J., WUNDER, F., STOCKER, M., LICHTINGHAGEN, R., MASTIAUX, F., BECKH, S., KUES, W., PEDARZANI, P., SCHROTER, K.H., RUPPERSBERG, J.P., VEH, R. & PONGS, O. (1992). Characterization of a *Shaw*-related potassium channel family in rat brain. *EMBO J.,* **11,** 2473–2486.

SANGUINETTI, M.C., JIANG, C.G., CURRAN, M.E. & KEATING, M.T. (1995). A mechanistic link between an inherited and an acquired cardiac arrythmia: HERG encodes the $IK_r$ potassium channel. *Cell,* **81,** 299–307.

SANGUINETTI, M.C., JOHNSON, J.H., HAMMERLAND, L.G., KELBAUGH, P.R., VOLKMANN, R.A., SACCOMANO, N.A. & MUELLER, A.L. (1997). Heteropodatoxins: peptides isolated from spider venom that block Kv4.2 potassium channels. *Mol. Pharmacol.,* **51,** 491–498.

SCHWEITZ, H. (1984). Lethal potency in mice of toxins from scorpion, sea anemone, snake and bee venoms following intraperitoneal and intracisternal injection. *Toxicon,* **22,** 308–311.

SCHWEITZ, H., BRUHN, T., GUILLEMARE, E., MOINIER, D., LANCELIN, J.-M., BÉRESS, L. & LAZDUNSKI, M. (1995). Kalicludines and Kaliseptine: two different classes of sea anemones toxins for voltage-sensitive K channels. *J. Biol. Chem.,* **270,** 25121–25126.

SEGAL, M., ROGAWSKI, M.A. & BARKER, J.L. (1984). A transient potassium conductance regulates the excitability of cultured hippocampal and spinal neurones. *J. Neurosci.,* **4,** 604–609.

SERODIO, P., KENTROS, C. & RUDY, B. (1994). Identification of molecular components of A-type channels activating at subthreshold potentials. *J. Neurophysiol.,* **72,** 1516–1529.

SERODIO, P. & RUDY, B. (1998). Differential expression of Kv4 K channel subunits mediating subthreshold transient K (A-type) currents in rat brain. *J. Neurophysiol.,* **79,** 1081–1091.

SERODIO, P., VEGA-SAENZ DE MIERA, E. & RUDY, B. (1996). Cloning of a novel component of A-type K channels operating at subthreshold potentials with unique expression in heart and brain. *J. Neurophysiol.,* **75,** 2174–2179.

STRONG, P.N. (1990). Potassium channel toxins. *Pharmacol. Ther.,* **46,** 137–162.

SWARTZ, K.J. & MCKINNON, R. (1997). Hanatoxin modifies the gating of a voltage-dependent K channel through multiple binding sites. *Neuron,* **18,** 665–673.

TSENG, G.N., JIANG, M. & YAO, J.A. (1996). Reverse use dependence of Kv4.2 blockade by 4-aminopyridine. *J. Pharmacol. Exp. Ther.,* **279,** 865–876.

TSENG-CRANK, J.C.L., TSENG, G.-N., SCHWARTZ, A. & TANOUYE, M.A. (1990). Molecular cloning and functional expression of a potassium channel cDNA isolated from a rat cardiac library. *FEBS Lett.,* **268,** 63–68.

WETTWER, E., AMOS, G.J., POSIVAL, H. & RAVENS, U. (1994). Transient outward current in human ventricular myocytes of subepicardial and subendocardial origin. *Circ. Res.,* **75,** 473–482.

YEOLA, S.W. & SNYDERS, D.J. (1997). Electrophysiological and pharmacological correspondence between Kv4.2 current and rat cardiac transient outward current. *Cardiovasc. Res.,* **33,** 540–547.

*(Received August 8, 1998*
*Revised October 1, 1998*
*Accepted October 9, 1998)*